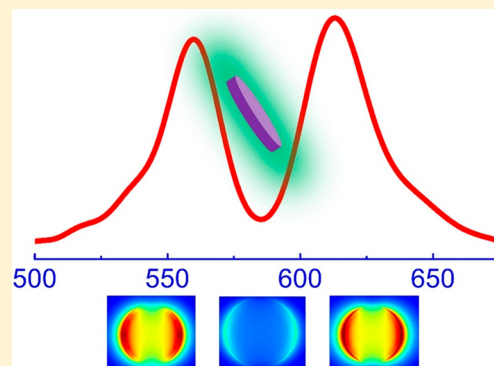


# Colloidal Nanodisk Shaped Plexcitonic Nanoparticles with Large Rabi Splitting Energies

Fadime Mert Balci,<sup>\*,†</sup> Sema Sarisozen,<sup>‡</sup> Nahit Polat,<sup>†</sup> and Sinan Balci<sup>\*,†</sup><sup>†</sup>Department of Photonics, Izmir Institute of Technology, Izmir 35430, Turkey<sup>‡</sup>Department of Chemistry, Izmir Institute of Technology, Izmir 35430, Turkey

## S Supporting Information

**ABSTRACT:** When plasmons supported by metal nanoparticles interact strongly with molecular excitons or excitons of semiconducting quantum dots, plexcitons are formed in the strong coupling regime. The hybrid plexcitonic nanoparticles with a wide range of sizes and shapes have been synthesized by using wet chemistry methods or have been fabricated on solid substrates by using lithographic techniques. In order to deeply understand plasmon–exciton interaction at the nanoscale dimension and boost the performance of nanophotonic devices made of plexcitonic nanoparticles, new types of plexcitonic nanoparticles with tunable optical properties and outstanding stability at room temperature are urgently needed. Herein, we for the first time report pure colloidal nanodisk shaped plexcitonic nanoparticles with very large Rabi splitting energies, i.e., more than 350 meV. We synthesize silver nanoprisms by using seed mediated synthesis and then convert nanoprisms to nanodisks at a high temperature. Localized plasmon resonance of the silver nanodisk in the visible spectrum can be effectively tuned by heating. Subsequently, self-assembly of J-aggregate dyes on plasmonic nanodisks produces plexcitonic nanoparticles. We envision that colloidal nanodisk shaped plexcitonic nanoparticles with very large Rabi splitting energies and outstanding stability at room temperature will enlarge the application of plexcitonic nanoparticles in a variety of fields such as polariton laser, biosensor, plasmon molecular nanodevices, and energy flow at nanoscale dimensions.



## INTRODUCTION

The recent advancements in nanofabrication and chemical synthesis of metal and semiconductor nanoparticles have allowed us to better control and understand light–matter interaction at nanoscale dimensions.<sup>1</sup> Metal nanoparticles tightly confining light at subwavelength dimensions because of generation of localized surface plasmon polaritons (SPPs) are good candidates for merging photonics and electronics at nanoscale dimensions.<sup>1–3</sup> When surface plasmons interact strongly with incoming photons, half-photon and half-electron hybrid states called SPPs are generated. Owing to the localization of incoming light into small volumes, enhancement of the field intensity compared to the incoming light, extreme sensitivity to size and shape of the supporting structure, and high sensitivity to the refractive index of the surrounding environment,<sup>4</sup> SPPs have found a variety of critical applications in areas such as surface enhanced spectroscopy, sensors, microscopy, nano-optics, solar cells, and light emitting diodes.<sup>5–7</sup> SPP enabled concentration of light into nanoscale volumes<sup>2</sup> has greatly enhanced the interaction of light with matter and boosted the performance of nanophotonic devices.<sup>4,8</sup>

In the strong coupling regime, metal nanoparticles supporting localized surface plasmon polaritons (quasiparticles) interact with excitons (quasiparticles) of molecules or quantum dots, and hence, new hybrid modes called plexcitons (plasmon–

exciton polaritons) are formed.<sup>9</sup> Compared with bare plasmon and exciton dispersion, the new system in the dispersion curve has lower and upper polariton branches, which are a clear indication of the strong coupling. In the strong coupling regime, excitons and plasmons are strongly coupled, and there is a reversible exchange of energy between them. Indeed, energy can reversibly flow back and forth between exciton and plasmon. It is noteworthy that, at zero detuning, the magnitude of the separation between the upper and lower branches is called a Rabi splitting energy.<sup>10</sup> Plexcitons are quasiparticles showing half-plasmonic and half-excitonic properties, and they have the best of two entirely different worlds, namely, plasmonics and excitonics. Furthermore, if plexcitons strongly interact with plasmons, new optical hybrid modes called plexcitons (plasmon–exciton–plasmon polaritons) are formed in the strong coupling regime.<sup>11,12</sup> Plexcitonic nanoparticles have been both fabricated on solid substrates by using new lithographic techniques and synthesized by using wet chemistry methods.<sup>13</sup> The first plexcitonic nanoparticles, synthesized by N. J. Halas et al., were gold nanoshell-J-aggregates with a Rabi splitting energy of 120 meV.<sup>9</sup> In another study, gold nanodisk dimers covered

Received: September 17, 2019

Revised: October 8, 2019

Published: October 11, 2019

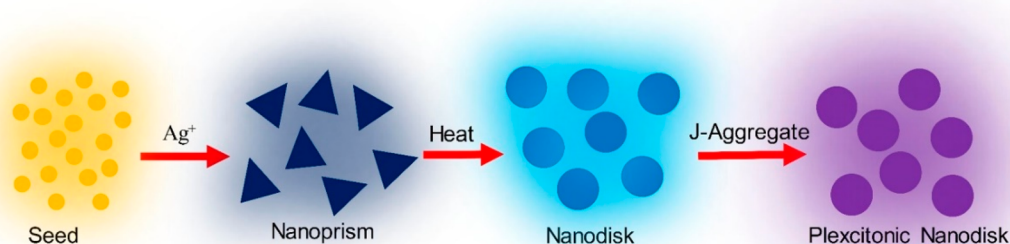


**Figure 1.** Schematic representation of the shape evolution of plasmonic nanoparticles and synthesis of plexcitonic nanodisks. Yellow colored silver seed nanoparticles are synthesized by reducing silver ions with a strong reducing agent, e.g., sodium borohydride. The seed mediated growth of the triangular silver nanoplate is accomplished by reducing silver ions in the presence of a weak reducing agent, e.g., ascorbic acid. The color of the nanoplate, i.e., the resonance wavelength of the colloid, is simply controlled by the number of seed nanoparticles in the reaction medium. Next, the initial silver nanoprisms are converted to silver nanodisks gradually by heating the nanoprism colloid at high temperature. In the final step, plasmonic nanodisks are transformed into plexcitonic nanodisks by introducing J-aggregate dyes, which self-assemble on the surface of silver nanodisks.

with a J-aggregate thin film on a solid substrate have been used for observing large Rabi splitting in individual metallic dimers,<sup>14</sup> and recently, they have been theoretically studied in detail.<sup>15</sup> Gold nanodisk arrays<sup>16</sup> and gold nanorod arrays<sup>17</sup> covered with a uniform thin film of J-aggregate molecules have been fabricated, and dynamic tuning of plasmon–exciton coupling has been elegantly demonstrated. Until now, a variety of differently shaped metal nanoparticles such as nanoprisms,<sup>18,19</sup> bipyramids,<sup>20</sup> nanorods,<sup>21</sup> spherical metal nanoparticles,<sup>22</sup> hollow gold nanoprisms,<sup>23</sup> and metal nanoparticle arrays<sup>24</sup> have been used to synthesize and fabricate plexcitonic nanoparticles.<sup>13</sup> Plexcitonic nanoparticles synthesized from nanoprism shaped silver nanoparticles have attracted a great amount of interest owing to the large Rabi splitting energy, availability in large quantities in aqueous media (colloid), easy detuning of the resonant frequency, large transparency dip in the extinction spectrum, and easy tuning of coupling strength.<sup>19,25–27</sup> In order to have a deeper and better understanding of the plasmon–exciton interaction at nanoscale dimensions and boost the performance of nanophotonic devices made of plexcitonic nanoparticles, a new type of plexcitonic nanoparticles with tunable optical properties and outstanding stability at room temperature are urgently needed. In this study, we for the first time report pure colloidal nanodisk shaped plexcitonic nanoparticles. Different from the previously published plexcitonic nanoparticle shapes, the new nanodisk shaped plexcitonic colloid has the following properties: (i) large Rabi splitting energy in the dispersion curve, (ii) large transparency dip in the extinction spectra, (iii) outstanding stability at room temperature, (iv) availability and pure form in large quantities, and (v) suitability for plexcitonic device applications. We synthesize silver nanoprisms by using seed mediated synthesis and then convert nanoprisms to nanodisks at high temperature. Localized plasmon resonance of the silver nanodisk in the visible spectrum can be effectively tuned by heating. Subsequently, plexcitonic nanoparticles are synthesized by self-assembling J-aggregate dyes on plasmonic nanodisks in the form of a colloidal suspension. The plexcitonic nanoparticle colloid contains only plexcitonic nanoparticles in aqueous medium but not any bare excitonic and plasmonic nanoparticles. We envision that colloidal nanodisk shaped plexcitonic nanoparticles with very large Rabi splitting energies, i.e., more

than 350 meV, will enlarge application of plexcitonic nanoparticles in a variety of fields such as plasmon laser, biosensor, solar cells, and plasmon molecular nanodevices.

## METHODS

Spherical silver nanoparticles were synthesized in an aqueous medium and used as the seed in the silver nanoprism synthesis, Figure 1. In a typical synthesis of silver seed nanoparticles, first, 5 mL of 2.5 mM trisodium citrate solution and 0.25 mL of 500 mg/L poly(sodium 4-styrenesulfonate) (PSS) were mixed with 0.3 mL of freshly prepared 10 mM NaBH<sub>4</sub>, i.e., a very good reducing agent. Afterward, 5 mL of 0.5 mM AgNO<sub>3</sub> was added drop by drop (~2 mL/min) in this solution combination under vigorous stirring. After about 30 min, a yellow colored silver nanoparticle colloid was obtained. Silver nanoprisms were synthesized by seed mediated synthesis as schematically shown in Figure 1. In a typical synthesis, first, 5 mL of Millipore water was mixed with 75 μL of 10 mM ascorbic acid, i.e., a weak reducing agent, and 60 μL of the seed solution. Afterward, 3 mL of 0.5 mM AgNO<sub>3</sub> was added drop by drop (~1 mL/min) in this solution combination under vigorous stirring. The color of the colloid first changes from yellow to red and then red to blue for nanoprisms having a resonance wavelength at around 700 nm. In the final stage, the Ag nanoprisms were stabilized by adding 0.5 mL of 25 mM trisodium citrate solution. It should be noted here that Millipore water was used throughout all experiments, and all the reactions were performed in aqueous medium at room temperature.

The shape conversion of silver nanoprisms was achieved by heating the silver nanoprisms as reported in earlier studies.<sup>28</sup> The as-synthesized silver nanoprism colloid was heated and stirred in an oil bath at 95 °C. The color of the silver nanoparticle colloid changed from blue to purple during the heating process. Subsequently, nanodisk shaped plexcitonic nanoparticles were synthesized by combining a silver nanodisk colloid with a J-aggregate dye. As a J-aggregate dye in this work, a cyanine dye, (5,5',6,6'-tetrachlorodi(4-sulfobutyl)benzimidazolocarbo-cyanine (TDBC) purchased from FEW Chemicals, was used without further purification. The nanodisk colloid was first centrifuged at 15 000 rpm for 15 min, and then, the supernatant was removed. This step can be repeated several times until all the reaction byproducts were completely removed. A 0.1 mM

TDBC dye solution with a varying amount was then added to the nanodisk colloid. In a typical experiment, varying amounts of 0.1 mM TDBC, e.g., 100 and 200  $\mu\text{L}$ , were added to 1 mL of the Ag nanodisk colloid. The uncoupled dye molecules must be removed from the reaction medium in order to obtain only plexcitonic nanoparticles. Therefore, uncoupled dye molecules were completely removed by centrifugation at 15 000 rpm for 15 min. The precipitate was redispersed in water, and spectroscopic investigations revealed that plasmons of metal nanoparticles and excitons of J-aggregates are strongly coupled. The size and shape of the silver nanoparticles were determined by using scanning transmission electron microscope (STEM) (Quanta 250, FEI). The silver nanoparticles were drop-cast on carbon coated copper grids. Extinction measurements of colloids were performed by using a balanced deuterium–tungsten halogen light source (DH2000-BAL, Ocean Optics), and a fiber coupled spectrometer (USB4000, Ocean Optics); see Supporting Information for the experimental setup.

The finite difference time domain (FDTD) method was employed to explore plasmon–exciton coupling in J-aggregate coated nanodisk shaped silver nanoparticles by using a commercial FDTD package from Lumerical. Silver nanodisk diameter and thickness were deduced from the STEM images. The electric field polarization is along the  $x$ -axis. Plane wave moves in the  $z$ -axis. The mesh size is 1 nm during the extinction spectra simulations and 0.1 nm during the electric field map simulations.

## RESULTS AND DISCUSSION

Silver nanoprisms (Ag NPs) were wet chemically synthesized in water by using seed mediated chemical synthesis of metal nanoparticles as reported in our previous works.<sup>18,19</sup> A two-step seed mediated chemical synthesis of metal nanoparticles was carried out; see Figure 1 for a schematic representation of the synthesis procedure. The isotropic and spherical Ag nanoparticles have a plasmon resonance wavelength at around 400 nm. The yellow color formation in silver seed synthesis is the strong indication of nanoparticle formation. In order to tune the resonance frequency of the silver nanoparticle in the visible spectrum, the size and shape of the nanoparticle must be changed since the plasmon resonance frequency of metal nanoparticles is very sensitive to the size, shape, and dielectric environment as well.<sup>29,30</sup> Actually, the higher number of seed nanoparticles in the reaction medium results in short edge lengths whereas the low number of seed nanoparticles results in long edge lengths. In fact, by controlling the amount of seed nanoparticle in the colloid, the plasmon resonance wavelength of the Ag nanoprism can be effectively tuned in the visible spectrum.<sup>18</sup>

After directly synthesizing silver nanoprisms, the shape of the nanoprisms was converted to nanodisks by heating, Figure 2a. There are several post-shape-conversion methods reported in the literature for controlling the shape of silver nanoparticles. Although initial shape conversion studies were based on converting spherical silver nanoparticles to nanoprisms, i.e., photoinduced conversion of silver nanospheres to nanoprisms,<sup>31</sup> later studies were mainly focused on conversion of nanoprisms to nanodisks.<sup>32</sup> These later studies mainly involve the following conclusions: (i) shape of the nanoprisms was converted to nanodisks;<sup>32</sup> (ii) localized surface plasmon resonance wavelength of the nanoparticles was tuned by heating;<sup>33</sup> (iii) a gradual blue-shift in the plasmon resonance bands of the nanoparticles was observed with heating;<sup>34</sup> (iv)

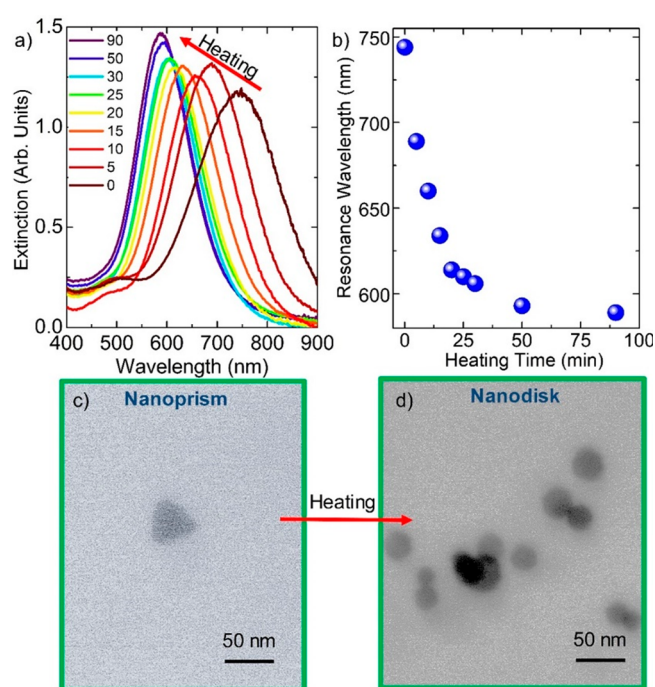


**Figure 2.** Nanodisk shaped plasmonic nanoparticles. (a) Evolution of extinction spectra of silver nanodisks under heating for 0–90 min. The initial silver nanoprisms with plasmon resonance wavelength of around 750 nm were converted into silver nanodisks at lower wavelengths. The red arrow indicates the direction of heating. (b) Plasmon resonance wavelength as a function of time. (c) STEM image of initial silver nanoprisms with edge length of around 45 nm. (d) STEM image of silver nanodisks after heating silver nanoprisms.

nanodisks were found to be more stable than nanoprisms;<sup>34</sup> (v) nanodisks and nanoprisms have a single-crystal structure;<sup>32</sup> and (vi) reversible shape conversion was achieved from nanoprisms to nanodisks, and vice versa.<sup>32</sup> Furthermore, silver nanoprisms were found to undergo shape transformation from nanoprism to nanodisk upon chemical functionalization by using thiol-terminated poly(ethylene glycol).<sup>35</sup> Here in this study, shape transformation was achieved by heating the triangular silver nanoplate colloid at 95 °C in an oil bath. Figure 2a shows the extinction spectra of a silver nanoprism colloid heated for 90 min. Initially, the localized plasmon resonance of the silver nanoprism is around 750 nm. After about 90 min of heating, the plasmon resonance wavelength is around 550 nm, Figure 2a. STEM images show that before heating plasmonic nanoparticles are triangular in shape and after heating the shape of the silver nanoparticles is mainly disk, Figure 2c,d, respectively. Indeed, truncation of the nanoprisms leads to the formation of nanodisks, Figure 3a. The evolution from silver nanoprism to nanodisk has been extensively studied in the literature, and it is assumed that silver atoms on the corner of the nanoprisms dissolve and reabsorb on the side of the silver nanoplates during the heating process.<sup>28</sup>

As a J-aggregate dye in this work, a cyanine dye, TDBC, was used for the synthesis of nanodisk shaped plexcitonic nanoparticles. The absorption spectrum of the dye shows a very clear and sharp exciton resonance at around 587 nm, see Figure 3b. Owing to the supramolecular self-assembly of individual dye molecules at a high concentration, the absorption band of the dye red-shifts to longer wavelengths with a very sharp resonance.<sup>36</sup> We then added various quantities of dye solution to silver nanodisk colloids under stirring to obtain hybrid



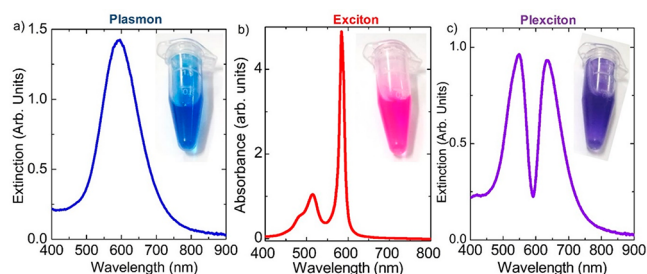


**Figure 3.** Nanodisk shaped plexcitonic nanoparticles. (a) Extinction spectrum of disk shaped silver nanoplate colloid in water. The plasmon resonance wavelength of the blue colored nanodisk shaped plasmonic nanoparticles is around 600 nm. The inset shows around 1 mL of the silver nanodisk colloid in a reaction vessel. (b) Absorption spectrum of TDBC dye in water. Individual TDBC molecules self-assemble at high concentration and generate J-aggregates having a sharp resonance at around 587 nm. The inset shows around 1 mL of aqueous solution of TDBC dye. (c) Extinction spectrum of disk shaped plexcitonic nanoparticle colloid. The purple colored colloid shows half-plasmonic and half-excitonic properties. The transparency dip at around 587 nm in the spectrum is indication of plexcitonic nanoparticle formation. The inset shows around 1 mL of the nanodisk shaped plexcitonic colloid.

metal–organic nanoparticles. The very sharp transparency dip in the extinction spectrum in Figure 3c is a very clear indication of plexcitonic nanoparticle formation. Indeed, individual dye molecules self-assemble on the surface of metal nanoparticles.<sup>19</sup> Uncoupled J-aggregate dyes in the solution were completely removed by centrifugation, and the pellet that formed after the centrifugation was resuspended in water. Therefore, the new colloid contains only plexcitonic nanoparticles.

In addition, we controlled the amount of dye molecules attached to metal nanoparticles by simply controlling the concentration of dye molecules in the reaction medium, Figure 4. In Figure 4a, a photo shows nanodisk colloids with varying concentrations of J-aggregate dyes. Evolution of extinction spectra of the nanodisk colloids with different Rabi splitting energies is shown in Figure 4b. When the energy transfer rate between exciton and plasmon,  $g$ , is larger than the plasmon decay rate,  $\kappa$ , and the exciton decay rate,  $\gamma$ , strong coupling of exciton and plasmon occurs ( $g \gg \gamma, \kappa$ ).<sup>37</sup> In this limit, there is a reversible exchange of energy between plasmons and excitons.<sup>38</sup> However, when the energy transfer rate is much smaller than the decay rates of plasmons and excitons ( $g \ll \gamma, \kappa$ ), weak coupling happens.<sup>10</sup> In Figure 4b, transition from the weak coupling regime to the strong coupling regime was observed. The calculated Rabi splitting energies increase with the square root of TDBC dye. It is noteworthy to state here that the strength of the plasmon–exciton coupling determined by the magnitude of the Rabi splitting energy was controlled with the amount of dye molecules in the medium.<sup>38</sup> In a classical description of coupled oscillators, the Rabi splitting frequency,  $\Omega$ , is proportional to the square root of the number of oscillators,  $(N)^{1/2}$  in the medium.<sup>10,11</sup> The calculated Rabi splitting energies, more than 350 meV, suggest that the coupled nanoparticles are indeed in the ultrastrong coupling regime.<sup>18</sup>

In order to deeply understand the plasmon–exciton coupling in silver nanodisk plexcitons, the polariton dispersion curve was plotted in Figure 5. It should be noted that the resonance frequency of the J-aggregate is not tunable whereas the resonance frequency of silver nanodisks is tunable by simply changing the size of the nanodisk. Therefore, the polariton dispersion curve was generated by tuning the resonance

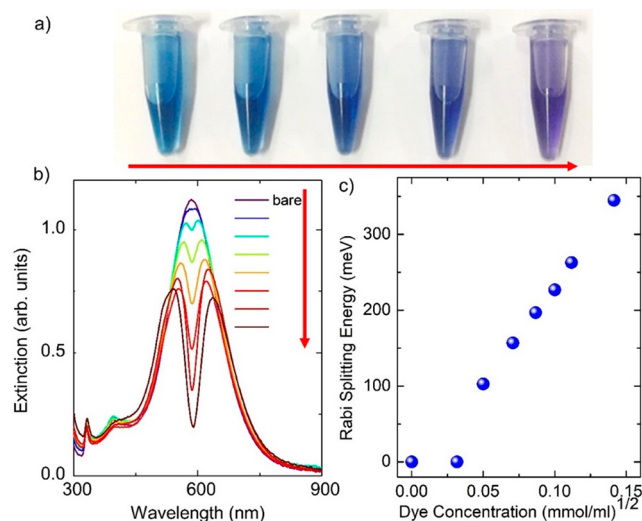


**Figure 4.** Tunable coupling in nanodisk shaped plexcitonic nanoparticles. (a) A photo of silver nanodisks, placed in a reaction vessel, coated with varying amount of J-aggregate dyes in water. (b) Evolution of extinction spectra of silver nanodisks with varying amount of J-aggregate dyes. Bare silver nanodisks were obtained by heating bare silver nanoprisms in water. (c) Calculated Rabi splitting energies from part b with a varying amount of J-aggregate dye coated onto the silver nanodisks. At a higher concentration of dye molecules, the Rabi splitting reaches saturation.

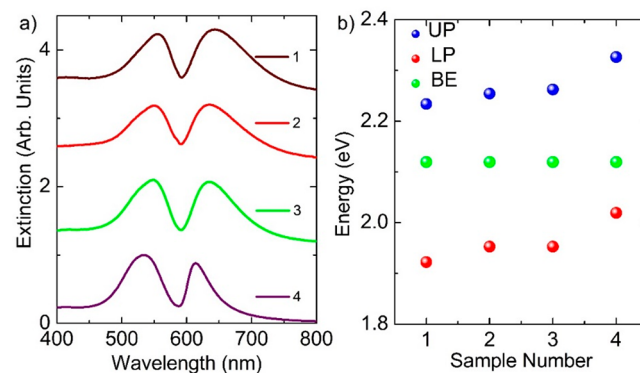


**Figure 5.** Polariton dispersion curve of nanodisk shaped plexcitonic nanoparticles. (a) Extinction spectra of nanodisk shaped plexcitonic nanoparticles synthesized from differently sized silver nanodisks. (b) The peak energies in part a are plotted as a function of the detuning. At the zero detuning, the calculated Rabi splitting energy is larger than 300 meV. In the figure, UP, LP, and BE represent the upper polariton branch, lower polariton branch, and bare exciton energy level, respectively. The bare plasmon band energy increases from the low sample number to the high sample number in the dispersion curve.

frequency of plasmonic nanoparticles. Figure 5a demonstrates the extinction spectra of nanodisk shaped plexcitonic nanoparticles synthesized from differently sized silver nanodisks. The calculated peak energies for each sample are plotted in Figure 5b. An avoided crossing appears when the plasmon resonance wavelength equals the bare exciton resonance wavelength, which corresponds to zero detuning. In fact, at the zero detuning, the Rabi splitting energy of larger than 300 meV can be calculated. By using the coupled oscillator model, the polariton dispersion curve can be modeled as  $E_{1,2}(k) = [E_{pl}(k) + E_{ex}]/2 \pm 1/2[(\hbar\Omega)^2 - (E_{pl}(k) - E_{ex})^2]^{1/2}$ , where  $k$  is the wave vector,  $E_1$  and  $E_2$  are the energies of the upper and lower polariton branches,  $E_{ex}$  is the

resonance energy of the bare exciton,  $E_{sp}$  is the energy of the bare surface plasmon, and  $\hbar\Omega$  is the Rabi splitting energy.<sup>10</sup>

To confirm the experimental results and further reveal the origin of the strong coupling between plasmon and exciton in the nanodisk shaped plexcitonic nanoparticle, FDTD simulation of a single plexcitonic nanoparticle was performed, Figure 6a. In

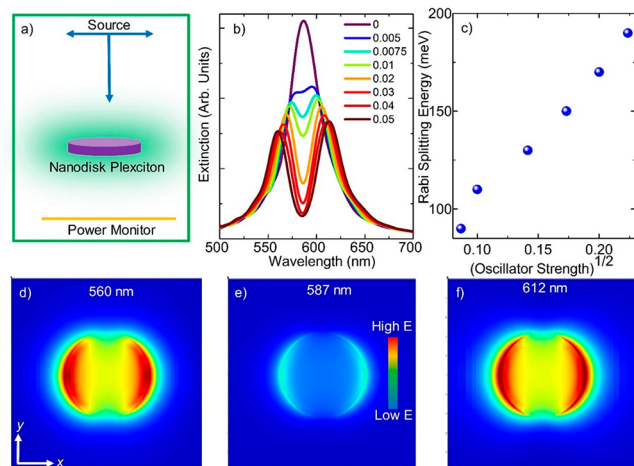


**Figure 6.** FDTD simulation of nanodisk shaped plexcitonic nanoparticle. (a) Schematic representation of FDTD simulation of single plexcitonic nanoparticle. Silver nanodisk was uniformly coated with a few nanometers thick J-aggregate dye. The simulation area is 60 nm × 60 nm. The electric field is polarized along the  $x$ -axis. The diameter of the nanodisk and thickness of the excitonic layer are 40 nm, and 1 nm, respectively. (b) Evolution of extinction spectra of single silver nanodisk with varying oscillator strength. Note that when the oscillator strength is zero, the single silver nanodisk is the bare plasmonic nanodisk. (c) Rabi splitting energy as a function of oscillator strength ranging from 0 to 0.05. Square root of oscillator strength increases linearly with the Rabi splitting energy. Electric field distribution of single plexcitonic nanoparticle at (d) 560 nm, (e) 587 nm, and (f) 612 nm. All plots share the same scale. Horizontal axis refers to the  $x$ -axis, whereas the vertical axis refers to the  $y$ -axis.

the simulation, the silver nanodisk was suspended in air (refractive index of 1.0), and we assumed that the dispersion of molecular exciton was Lorentzian, which was expressed as  $\epsilon(\omega) = \epsilon_{\infty} + f_0(\omega_0^2/(\omega_0^2 - \omega^2 - i\gamma_0\omega))$  where the resonance wavelength of the J-aggregate was set to 587 nm (2.11 eV), and the width of the molecular exciton resonance ( $\gamma_0$ ) was set to around 32 meV. The background index,  $\epsilon_{\infty}$ , was set to 2.1. The oscillator strength of the J-aggregate ( $\gamma_0$ ) was set to vary from 0 to 0.05, Figure 6b. There is an excellent qualitative agreement between the experimental results and FDTD simulations, see Figure 6c and Figure 4c. The origin of the large Rabi splitting energy observed in the silver nanodisk is the high electric field localization around the nanoparticle at resonance conditions. Figure 6d–f shows the electric field distribution of a single plexcitonic nanoparticle at 560, 587, and 612 nm, respectively. The induced transparency as a narrow dip in the extinction spectra where the electric field intensity is close to zero (at around 587 nm) is a very strong indication of plexciton formation. Note that the bare silver nanodisk at the same frequency has very large electric field localization, see Supporting Information.

## CONCLUSIONS

In summary, we for the first time report pure colloidal nanodisk shaped plexcitonic nanoparticles with very large Rabi splitting energies, i.e., more than 350 meV. We synthesize silver nanoprisms by using seed mediated synthesis and then convert nanoprisms to nanodisks at high temperature where nanoprism to nanodisk shape conversion was achieved through dissolution and reabsorption of silver ions on the surface of silver nanoprisms. Resonance frequency of the plasmonic nanodisks can be effectively tuned by heating the silver colloid in the visible spectrum. Subsequently, pure colloidal plexcitonic nanoparticles are synthesized by self-assembling of J-aggregate dyes on plasmonic nanodisks. In the strong coupling regime, half-plasmonic and half-excitonic hybrid nanodisk shaped plexcitonic nanoparticles are generated. The experimental results corroborated well with the theoretical simulation of single plexcitonic and plasmonic shaped nanoparticles. The plexcitonic nanodisks are stable in aqueous solution and can be stored at room temperature for several weeks. We envision that nanodisk shaped plexcitonic nanoparticles with very large Rabi splitting energies and outstanding stability at room temperature will enlarge application of plexcitonic nanoparticles in a variety of fields such as plasmon laser, biosensor, solar cells, and molecular nanophotonics active devices.<sup>1</sup> The plexcitonic colloid can be used to fabricate a variety of nanophotonic devices for understanding energy flow (plexciton propagation) at nanoscale dimensions.<sup>1,3,4</sup> In addition, large area plexcitonic devices can be easily fabricated and integrated with two-dimensional nanomaterials such as graphene, owing to the availability of a large amount of pure colloidal plexcitonic nanoparticle colloid.<sup>39</sup>

## ASSOCIATED CONTENT

### Supporting Information

The Supporting Information is available free of charge on the ACS Publications website at DOI: 10.1021/acs.jpcc.9b08834.

STEM images of silver nanodisks, extinction spectrum of silver seed nanoparticles, absorbance spectrum of TDBC in aqueous solution, extinction spectra of silver nanodisks under heating, FDTD simulation of plexcitonic and plasmonic nanodisks, schematic representation of UV–vis spectrophotometer, and dielectric function of Lorentz oscillator (PDF)

## AUTHOR INFORMATION

### Corresponding Authors

\*E-mail: fmertbalci@fen.bilkent.edu.tr.

\*E-mail: sinanbalci@iyte.edu.tr.

### ORCID

Sinan Balci: 0000-0002-9809-8688

### Notes

The authors declare no competing financial interest.

## ACKNOWLEDGMENTS

This research was partially supported by the Scientific and Technological Research Council of Turkey (TUBITAK) (Grants 118F066 117F172).

## REFERENCES

(1) Yuen-Zhou, J.; Saikin, S. K.; Zhu, T.; Onbasli, M. C.; Ross, C. A.; Bulovic, V.; Baldo, M. A. Plexciton Dirac Points and Topological Modes. *Nat. Commun.* **2016**, *7*. DOI: 10.1038/ncomms11783

- (2) Barnes, W. L.; Dereux, A.; Ebbesen, T. W. Surface Plasmon Subwavelength Optics. *Nature* **2003**, *424*, 824–830.
- (3) Ozbay, E. Plasmonics: Merging Photonics and Electronics at Nanoscale Dimensions. *Science* **2006**, *311*, 189–193.
- (4) Pala, R. A.; White, J.; Barnard, E.; Liu, J.; Brongersma, M. L. Design of Plasmonic Thin-Film Solar Cells with Broadband Absorption Enhancements. *Adv. Mater.* **2009**, *21*, 3504.
- (5) Aslan, K.; Wu, M.; Lakowicz, J. R.; Geddes, C. D. Fluorescent Core-Shell Ag@SiO<sub>2</sub> Nanocomposites for Metal-Enhanced Fluorescence and Single Nanoparticle Sensing Platforms. *J. Am. Chem. Soc.* **2007**, *129*, 1524.
- (6) Sherry, L. J.; Jin, R. C.; Mirkin, C. A.; Schatz, G. C.; Van Duyne, R. P. Localized Surface Plasmon Resonance Spectroscopy of Single Silver Triangular Nanoprisms. *Nano Lett.* **2006**, *6*, 2060–2065.
- (7) Odom, T. W.; Schatz, G. C. Introduction to Plasmonics. *Chem. Rev.* **2011**, *111*, 3667–3668.
- (8) Ebbesen, T. W.; Lezec, H. J.; Ghaemi, H. F.; Thio, T.; Wolff, P. A. Extraordinary Optical Transmission through Sub-Wavelength Hole Arrays. *Nature* **1998**, *391*, 667–669.
- (9) Fofang, N. T.; Park, T. H.; Neumann, O.; Mirin, N. A.; Nordlander, P.; Halas, N. J. Plexcitonic Nanoparticles: Plasmon-Exciton Coupling in Nanoshell-J-Aggregate Complexes. *Nano Lett.* **2008**, *8*, 3481–3487.
- (10) Balci, S.; Kocabas, C.; Ates, S.; Karademir, E.; Salihoglu, O.; Aydinli, A. Tuning Surface Plasmon-Exciton Coupling Via Thickness Dependent Plasmon Damping. *Phys. Rev. B: Condens. Matter Mater. Phys.* **2012**, *86*. DOI: 10.1103/PhysRevB.86.235402
- (11) Balci, S.; Kocabas, C. Ultra Hybrid Plasmonics: Strong Coupling of Plexcitons with Plasmon Polaritons. *Opt. Lett.* **2015**, *40*, 3424–3427.
- (12) Yang, H.; Yao, J.; Wu, X. W.; Wu, D. J.; Liu, X. J. Strong Plasmon-Exciton-Plasmon Multimode Couplings in Three-Layered Ag-J-Aggregates-Ag Nanostructures. *J. Phys. Chem. C* **2017**, *121*, 25455–25462.
- (13) Baranov, D. G.; Wersall, M.; Cuadra, J.; Antosiewicz, T. J.; Shegai, T. Novel Nanostructures and Materials for Strong Light Matter Interactions. *ACS Photonics* **2018**, *5*, 24–42.
- (14) Schlather, A. E.; Large, N.; Urban, A. S.; Nordlander, P.; Halas, N. J. Near-Field Mediated Plexcitonic Coupling and Giant Rabi Splitting in Individual Metallic Dimers. *Nano Lett.* **2013**, *13*, 3281–3286.
- (15) Kondorskiy, A. D.; Lebedev, V. S. Spectral-Band Replication Phenomenon in a Single Pair of Hybrid Metal-Organic Nanospheres and Nanodisks Caused by Plexcitonic Coupling. *Opt. Express* **2019**, *27*, 11783–11799.
- (16) Zheng, Y. B.; Juluri, B. K.; Jensen, L. L.; Ahmed, D.; Lu, M. Q.; Jensen, L.; Huang, T. J. Dynamic Tuning of Plasmon-Exciton Coupling in Arrays of Nanodisk-J-Aggregate Complexes. *Adv. Mater.* **2010**, *22*, 3603.
- (17) Wurtz, G. A.; Evans, P. R.; Hendren, W.; Atkinson, R.; Dickson, W.; Pollard, R. J.; Zayats, A. V.; Harrison, W.; Bower, C. Molecular Plasmonics with Tunable Exciton-Plasmon Coupling Strength in J-Aggregate Hybridized Au Nanorod Assemblies. *Nano Lett.* **2007**, *7*, 1297–1303.
- (18) Balci, S. Ultrastrong Plasmon-Exciton Coupling in Metal Nanoprisms with J-Aggregates. *Opt. Lett.* **2013**, *38*, 4498–4501.
- (19) Balci, S.; Kucukoz, B.; Balci, O.; Karatay, A.; Kocabas, C.; Yaglioglu, G. Tunable Plexcitonic Nanoparticles: A Model System for Studying Plasmon-Exciton Interaction from the Weak to the Ultrastrong Coupling Regime. *ACS Photonics* **2016**, *3*, 2010–2016.
- (20) Stuhrenberg, M.; Munkhbat, B.; Baranov, D. G.; Cuadra, J.; Yankovich, A. B.; Antosiewicz, T. J.; Olsson, E.; Shegai, T. Strong Light-Matter Coupling between Plasmons in Individual Gold Bi-Pyramids and Excitons in Mono- and Multilayer Wse<sub>2</sub>. *Nano Lett.* **2018**, *18*, 5938–5945.
- (21) Zengin, G.; Johansson, G.; Johansson, P.; Antosiewicz, T. J.; Kall, M.; Shegai, T. Approaching the Strong Coupling Limit in Single Plasmonic Nanorods Interacting with J-Aggregates. *Sci. Rep.* **2013**, *3*. DOI: 10.1038/srep03074
- (22) Lekeufack, D. D.; Brioude, A.; Coleman, A. W.; Miele, P.; Bellessa, J.; Zeng, L. D.; Stadelmann, P. Core-Shell Gold J-Aggregate Nanoparticles for Highly Efficient Strong Coupling Applications. *Appl. Phys. Lett.* **2010**, *96*, 253107.
- (23) Das, K.; Hazra, B.; Chandra, M. Exploring the Coherent Interaction in a Hybrid System of Hollow Gold Nanoprisms and Cyanine Dye J-Aggregates: Role of Plasmon-Hybridization Mediated Local Electric-Field Enhancement. *Phys. Chem. Chem. Phys.* **2017**, *19*, 27997–28005.
- (24) Zakharko, Y.; Rother, M.; Graf, A.; Hahnlein, B.; Brohmann, M.; Pezoldt, J.; Zaumseil, J. Radiative Pumping and Propagation of Plexcitons in Diffractive Plasmonic Crystals. *Nano Lett.* **2018**, *18*, 4927–4933.
- (25) Wersall, M.; Cuadra, J.; Antosiewicz, T. J.; Balci, S.; Shegai, T. Observation of Mode Splitting in Photoluminescence of Individual Plasmonic Nanoparticles Strongly Coupled to Molecular Excitons. *Nano Lett.* **2017**, *17*, 551–558.
- (26) DeLacy, B. G.; et al. Coherent Plasmon-Exciton Coupling in Silver Platelet-J-Aggregate Nanocomposites. *Nano Lett.* **2015**, *15*, 2588–2593.
- (27) Munkhbat, B.; Wersall, M.; Baranov, D. G.; Antosiewicz, T. J.; Shegai, T. Suppression of Photo-Oxidation of Organic Chromophores by Strong Coupling to Plasmonic Nanoantennas. *Sci. Adv.* **2018**, *4*, eaas9552.
- (28) Tang, B.; Xu, S. P.; Hou, X. L.; Li, J. H.; Sun, L.; Xu, W. Q.; Wang, X. G. Shape Evolution of Silver Nanoplates through Heating and Photoinduction. *ACS Appl. Mater. Interfaces* **2013**, *5*, 646–653.
- (29) Jin, R. C.; Cao, Y. C.; Hao, E. C.; Mettraux, G. S.; Schatz, G. C.; Mirkin, C. A. Controlling Anisotropic Nanoparticle Growth through Plasmon Excitation. *Nature* **2003**, *425*, 487–490.
- (30) Kelly, K. L.; Coronado, E.; Zhao, L. L.; Schatz, G. C. The Optical Properties of Metal Nanoparticles: The Influence of Size, Shape, and Dielectric Environment. *J. Phys. Chem. B* **2003**, *107*, 668–677.
- (31) Jin, R. C.; Cao, Y. W.; Mirkin, C. A.; Kelly, K. L.; Schatz, G. C.; Zheng, J. G. Photoinduced Conversion of Silver Nanospheres to Nanoprisms. *Science* **2001**, *294*, 1901–1903.
- (32) Tang, B.; An, J.; Zheng, X. L.; Xu, S. P.; Li, D. M.; Zhou, J.; Zhao, B.; Xu, W. Q. Silver Nanodisks with Tunable Size by Heat Aging. *J. Phys. Chem. C* **2008**, *112*, 18361–18367.
- (33) Chen, S. H.; Fan, Z. Y.; Carroll, D. L. Silver Nanodisks: Synthesis, Characterization, and Self-Assembly. *J. Phys. Chem. B* **2002**, *106*, 10777–10781.
- (34) Zhang, Q.; Ge, J. P.; Pham, T.; Goebel, J.; Hu, Y. X.; Lu, Z.; Yin, Y. D. Reconstruction of Silver Nanoplates by Uv Irradiation: Tailored Optical Properties and Enhanced Stability. *Angew. Chem., Int. Ed.* **2009**, *48*, 3516–3519.
- (35) Liu, L. J.; Burnyeat, C. A.; Lepsenyi, R. S.; Nwabuko, I. O.; Kelly, T. L. Mechanism of Shape Evolution in Ag Nanoprisms Stabilized by Thiol-Terminated Poly(Ethylene Glycol): An in Situ Kinetic Study. *Chem. Mater.* **2013**, *25*, 4206–4214.
- (36) Jelley, E. E. Spectral Absorption and Fluorescence of Dyes in the Molecular State. *Nature* **1936**, *138*, 1009–1010.
- (37) Tischler, J. R.; Bradley, M. S.; Zhang, Q.; Atay, T.; Nurmikko, A.; Bulovic, V. Solid State Cavity Qed: Strong Coupling in Organic Thin Films. *Org. Electron.* **2007**, *8*, 94–113.
- (38) Vasa, P.; Lienau, C. Strong Light-Matter Interaction in Quantum Emitter/Metal Hybrid Nanostructures. *ACS Photonics* **2018**, *5*, 2–23.
- (39) Balci, S.; Balci, O.; Kakenov, N.; Atar, F. B.; Kocabas, C. Dynamic Tuning of Plasmon Resonance in the Visible Using Graphene. *Opt. Lett.* **2016**, *41*, 1241–1244.